

MICROSTRUCTURAL PROPERTIES OF NEUTRON IRRADIATED FE-CR-C ALLOYS

T. Brodziansky¹, V. Slugeň¹, M. J. Konstantinovič²

¹Institute of Nuclear and Physical Engineering, Faculty of Electrical Engineering and Information Technology, Slovak University of Technology in Bratislava, Ilkovičova 3, 812 19 Bratislava, Slovak Republic, ² Studiecentrum voor Kernenergie/Centre d'Etude de l'Energie Nucléaire (SCK·CEN), Boeretang 200, B-2400 Mol, Belgium

E-mail: tomas.brodziansky@stuba.sk

Received 30 April 2017; accepted 14 May 2017

1. Introduction

Ferritic/martensitic (F/M) high-Cr steels are candidate structural materials for the construction of several components of future Generation IV (GEN IV) reactors, because they are more resistant to irradiation than stainless steels, while offering good thermal and thermal-mechanical properties. Still, despite accumulated research [1–4], the perception on the role that the different alloying elements and their amount have on the mechanical performance of these steels under irradiation is limited. Moreover, the influence of the initial microstructure of 9Cr steels and alloys on the defect properties formed after irradiation, and their overall contribution to the degradation of the mechanical properties, is not yet fully understood. The 9Cr steels are preferred mainly on the basis of the fact that they seem to offer a good compromise between corrosion resistance and minimal toughness degradation/reduced shift of ductile-brittle transition temperature [5, 6], while being more resistant to swelling than stainless steels. One of the main parameters which are responsible for the variation of the alloy microstructure and defect properties after irradiation is dissolved carbon distribution. Carbon easily segregates at dislocations and grain boundaries as well as it binds to neutron irradiation induced defects such as vacancy and interstitial clusters and precipitates [7]. These nano-metric complexes obstruct dislocation motion, thereby inducing the hardening and consequently causing embrittlement.

In this study, the Fe-Cr-C alloys with different Cr and C concentrations are investigated to study the influence of the interplay between ferritic and ferritic/martensitic phases to the defect properties in these alloys after neutron irradiation.

2. Sample preparation

Materials

Fe-Cr-C alloys were fabricated by vacuum induction furnace melting of industrial Fe (containing carbon) and appropriate amount of various solutes (added as pure elements) required to reach desired chemical composition. The impurity level is kept below 100 ppm. After casting, the materials were introduced in a pre-heated furnace to about 1200°C and hot rolled. The sheets were subsequently air-cooled down to room temperature. Besides Fe-Cr alloys, two 9Cr steels were investigated. The first one is the commercially available ferritic/martensitic steel T91 while the second is the European Reduced Activation Ferritic Martensitic (RAFM) steel EUROFER97 thereafter indicated as EUROFER97 or E97. E97 was delivered to SCK-CEN from FZK (Germany) and the T91 from CEA/Saclay (France) [8].

Specimen preparation consisted of surface polishing to a mirror finish with 1µm diamond paste and chemical etching by HF+H₂O₂+H₂O solution to remove deformed surface layer (~0.05 mm).

Tab. 1. *Chemical composition of the alloys (wt%).*

Material	C	Cr	N	Si	P	Ni	S	Al
Fe*	< 0.005	0.002	< 0.005	0.001	0.003	0.007	< 0.005	0.023
Fe-5Cr-NiSiP		4.9		0.219	0.033	0.097		0.026
Fe-9Cr (F)		9.1		0.004	0.003	0.009		0.027
Fe-9Cr-NiSiP		9.1		0.212	0.032	0.092		0.028
Fe-14Cr-NiSiP		14.4		0.194	0.031	0.087		0.025

Material	C	Cr	N	Si	P	Ni	V	Mn	S	Ti	Al	O
Fe-9Cr (F/M.)	0.02	8.4	0.015	0.09	0.012	0.07	0.002	0.03	0.0007	0.0034	0.0069	0.066

Material	C	Cr	N	Si	P	Ni	V	Ta	W	Mn	Mo
E97 (F/M)	0.12	8.96	0.016	0.07	<0.005	0.07	0.19	0.13	1.1	0.43	-
T91 (F/M)	0.1	8.32	0.03	0.32	0.02	0.24	0.24	-	<0.01	0.43	0.96

Neutron irradiation

Neutron irradiation was performed in the Belgian nuclear reactor 2 (BR2) of SCK•CEN in Mol. The irradiation conditions are presented in Table 2. The neutron flux was around 7.4×10^{13} n/cm²/s. Taking into account the results of the dosimetry, that depend on the power of the reactor and the neutron spectrum, the fluence in the range of $6.5-7.5 \times 10^{19}$ n/cm² was reached. Small variation of the fluence which occurred due to the gradient of neutron flux is neglected, and the fluence for all samples is calculated to correspond to 0.11 dpa.

3. Experimental technique

Positron Annihilation Spectroscopy (PAS) is a powerful tool for characterizing microstructural changes in materials after neutron irradiation. PAS is particularly sensitive to open volume defects, such as vacancies, vacancy clusters and dislocations. The sensitivity range for the vacancy detection in metals starts at about one vacancy per 107 atoms [9]. It is the only method providing information about vacancy clusters evolution under irradiation.

Coincidence Doppler Broadening Spectroscopy

In order to minimize the background, the CDB spectra were measured using two Ge detectors located at an angle of 180° relative to each other that allows both annihilation photons to be detected coincidentally. Details of the setup are described elsewhere [10]. To prevent pileup, due to the activity of the specimens, the detectors could be moved further from specimen (up to 1.5m).

The analysis of the results is based on channel selection through the coincidence region of the two-dimensional (2-D) spectra. The resulting 1-D spectrum was normalized to pure, non-irradiated, defect free iron.

Doppler broadening spectra is characterized by an S parameter (line-shape parameter) and a W parameter (wing parameter). These two parameters are extracted from each spectrum and they are defined as the ratio of low momentum ($|p_L| < 2.5 \times 10^{-3} m_0 c$) and high momentum ($15 \times 10^{-3} m_0 c < |p_L| < 25 \times 10^{-3} m_0 c$) regions of the CDB spectrum to total momentum respectively (c – speed of light, p_L - longitudinal component of the positron-electron momentum along the direction of γ -ray emission). S and W parameters carry different information. Annihilation with the valence electrons lead to a small difference in the energy of γ -rays, while the inner shell electrons can lead to energy changes of any magnitude. The former contributes to the low-momentum region and is observed by the S parameter, which therefore carries information about open volume defects. The latter, on the other hand,

contributes to the high-momentum region represented by W parameter. Therefore, the changes in the γ -ray energies due to inner shell electrons carries information on the chemical environment of annihilation sites [11].

4. Results and discussion

Measured materials could be divided into 3 groups according to initial microstructure: specimens Fe, Fe-5Cr-NiSiP, Fe-9Cr (F), Fe-9Cr-NiSiP, Fe-14Cr-NiSiP are ferritic Fe-Cr-C alloys, specimen Fe-9Cr (F/M) is ferritic/martensitic Fe-Cr-C alloy and specimens E97 and T91 are ferritic/martensitic steels. Structure of these dual-phase materials consists of ferrite matrix containing martensitic laths that are created during quenching in prior austenitic grains.

Non-irradiated

The results of the CDB measurements for non-irradiated materials are given in Figure 1a, where the W parameter is plotted as a function of S parameter for all alloys and steels, including the data for pure Fe. This figure indicates that steels exhibit somewhat higher S parameter and lower W parameter compared to the Fe-Cr-C alloys (since the total amount of annihilating positrons is fixed, in general an increase of S is necessarily accompanied by decrease of W), i.e. containing more vacancy type defects. This is probably due to the fact that they have more complex chemical composition and higher dislocation density. Another factor that could affect the S parameter is the microstructure of the materials, as could be seen in Figure 1a, where all three materials with ferritic/martensitic microstructure exhibit higher values of the S parameter compared to ferritic materials. Pure ferritic microstructure has the lowest concentration of open volume defects associated with low angle grain boundaries with respects to alloys with ferritic/martensitic microstructure. For example, in spite of almost the same Cr concentration, the Fe-9Cr (F) alloy and Fe-9Cr (F/M) alloy exhibit ferritic and ferritic/martensitic microstructure due to large difference in carbon content, see Tab. 1.

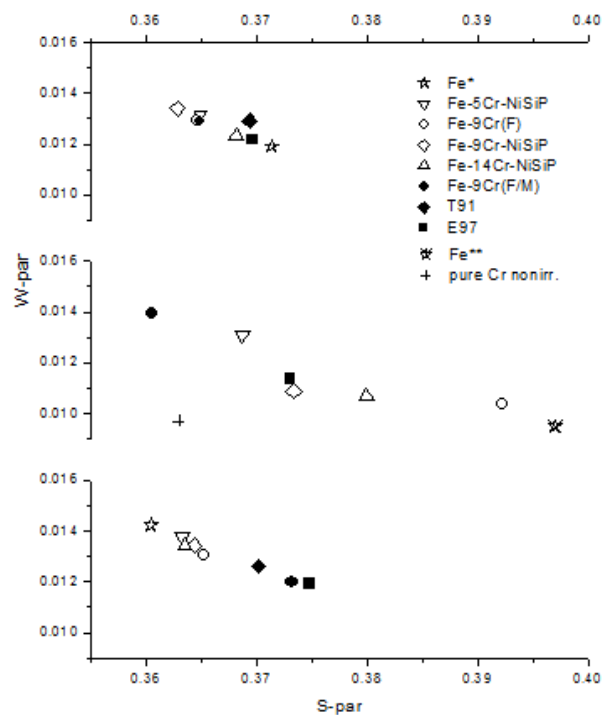


Fig. 1: W parameter as function of the S parameter for the non-irradiated state (a), irradiation at 290°C (b) and irradiation at 450°C (c); pure Cr non-irradiated is added only for comparison.

Irradiation at $T = 290^{\circ}\text{C}$

All materials irradiated at 290°C (Figure 1b), exhibit an increase of the S parameter and a decrease of the W parameter compared to the non-irradiated condition. In general, the S parameter can be affected by both the number density and the size of vacancy-type defects [12], so this enhancement of the S parameter indicates that positrons are trapped and annihilate at vacancy-rich complexes induced by neutron irradiation.

The most interesting observation is the change of the S parameter of the specimens Fe-9Cr (F) and Fe-9Cr (F/M) after being irradiated at 290°C (Fig. 2) compared to the non-irradiated state (Fig. 1a). In the non-irradiated case, ferritic/martensitic Fe-9Cr (F/M) exhibit more open volume defects than Fe-9Cr (F) with pure ferritic microstructure. In the contrary, after irradiation at 290°C opposite behavior occurs and specimen Fe-9Cr (F) has significantly more open volume defects than Fe-9Cr (F/M). This results indicates that initial microstructure of alloys, in particular dissolved carbon distribution, plays an important role in terms of defects evolution after neutron irradiation. It is known from accumulated research that carbon and vacancies strongly interact and form stable carbon-vacancy (CVa) complexes such as CVa, C_2Va , C_4Va_2 and bigger ones. These complexes act as traps for gliding interstitial dislocation loops and vacancies, thereby preventing them from reaching sinks (grain boundaries and dislocations) [13, 14, 15]. Internal friction (IF) and magnetic after-effect (MAE) studies revealed that, as manifestation of the different initial microstructure, C atoms were distributed differently within the matrix of the pure ferritic vs. ferritic/martensitic alloys [6]. Namely, while in the ferritic alloy most of the C atoms were distributed uniformly within the matrix, in ferritic/martensitic alloy the matrix was virtually free of C, where most of it had segregated at the martensite lath boundaries and grain boundaries. So, in the case of ferritic/martensitic Fe-9Cr (F/M) alloy irradiation induced defects, especially vacancies, easily glide towards sinks such as grain boundaries and lath boundaries. While in the case of ferritic Fe-9Cr (F) alloy, these irradiation induced vacancies stick to C atoms, which are uniformly distributed in the matrix and ready to interact with irradiation defects, creating very strong and stable CVa defects with high dissociation energies, e.g. as established from the DFT calculations for a vacancy-carbon pair it's 1.12 eV. Because of formation of these CVa complexes, which prevent irradiation induced vacancies from gliding and reaching the sinks, combined with relatively low migration energy of a single vacancy (~ 0.64 eV from DFT calculations) [17] compared to migration energy of CVa complexes, new vacancies are easily attached and therefore promoting vacancy cluster to grow. Therefore this might be the explanation for the relatively high increase of the S parameter in Fe-9Cr (F) compared to Fe-9Cr (F/M).

In general, the lowest value of the S parameter is observed in ferritic/martensitic Fe-9Cr (F/M) alloy, while alloys with comparatively same amount of Cr, but with pure ferritic microstructure (Fe-9Cr (F), Fe-9Cr-NiSiP) exhibit higher values of the S parameter. Ferritic alloys Fe-5Cr-NiSiP, Fe-9Cr-NiSiP and Fe-14Cr-NiSiP exhibit lower values of the S parameter which means that they contains less open volume defects than other ferritic alloy Fe-9Cr (F). Decrease of the S parameter occurred because of more complex chemical composition of the alloys Fe-5Cr-NiSiP, Fe-9Cr-NiSiP and Fe-14Cr-NiSiP, containing more solute atoms than Fe-9Cr (F) which act as additional sinks for irradiation induced vacancies to recombine. Alloys Fe-9Cr-NiSiP and Fe-14Cr-NiSiP exhibit a significant decrease of the W parameter in comparison with the trend in other alloys which is caused by increasing level of Cr, Nagai *et al.* showed that Cr itself has chemical effect in the sense of increasing S and decreasing W [18]. This deviation from the trend-straight line towards the point of pure non-irradiated Cr (Fig. 1b, added only for illustration) indicates the presence of Cr-rich solute clusters caused by irradiation accelerated phase separation between an iron rich phase (α) and chromium rich (α') phase.

Irradiation at $T = 450^{\circ}\text{C}$

The results of the CDB measurements for alloys irradiated at 450°C are given in Figure 1c. As could be seen from the figure, values of the S parameter practically decreased to level of non-irradiated alloys. Also the significant difference in S parameter of ferritic Fe-9Cr(F) alloy and ferritic/martensitic Fe-9Cr(F/M) alloy from the Fig. 1b has vanished and both exhibit almost identical values of the S parameter. This general decrease of the S parameter and equaling the values of S parameter for Fe-9Cr(F) and Fe-9Cr(F/M) alloys after irradiation at high temperatures may present another confirmation of the theory that the evolution of open volume defects after neutron irradiation is highly dependent on the initial microstructure, in particular dissolved carbon distribution, since as reported by various authors CVa complexes dissolve at $400\text{-}430^{\circ}\text{C}$ [13, 16]. If irradiation is performed above this temperature, dissociation of highly stable and immobile CVa complexes occurs and irradiation induced vacancies are not trapped therefore could easily migrate towards the sinks and disappear – no vacancy clustering occurs.

5. Summary and conclusion

In this work, neutron irradiated Fe-Cr-C alloys with various Cr concentration ($\sim 5\%$, $\sim 9\%$ and $\sim 14\%$ Cr) and different initial microstructure (pure ferritic and ferritic/martensitic) which is characterized by a different distribution of C atoms in the matrix have been investigated by CDBS measurements. It turns out that values of the S parameter, which corresponds to number density/size of the open volume defects, is higher for the alloys with pure ferritic than alloys with ferritic/martensitic initial microstructure after the irradiation to 0.11 dpa at 290°C . Based on the results, an important correlation between initial microstructure, in particular dissolved carbon distribution, and evolution of vacancy type defects after neutron irradiation could be highlighted. The presence of C atoms in a ferritic microstructure promotes the formation of vacancy clusters in the investigated alloys due to the formation of stable and immobile CVa complexes which act as traps for irradiation induced vacancies and prevent them from reaching the sinks, therefore these vacancies could coalesce and create vacancy clusters. On the contrary, alloys with ferritic/martensitic initial microstructure exhibit lower S parameter values suggesting suppressed formation of vacancy clusters due to the absence of C atoms in the matrix (C atoms are segregated at lath/grain boundaries) and inability to create CVa complexes. This theory is also supported by the CDBS results from alloys irradiated to 0.11 dpa at 450°C , where all alloys independently on initial microstructure exhibit S parameter values comparable to non-irradiated condition caused by the dissociation of stable CVa complexes at such high irradiation temperature. This suggest that the presence of C atoms in the matrix may counteract the positive effect of Cr in terms of swelling suppression for neutron irradiation at temperatures below $\sim 400 - 430^{\circ}\text{C}$. At this temperature, dissociation of CVa complexes occurs and C doesn't play role in terms of void formation anymore.

Acknowledgement

Authors acknowledge VEGA grants 1/0104/17. 1/0447/16 and 1/339/16

References:

- [1] E.A. Little, R. Bullough, M.H. Wood, *Proc. R. Soc. London A* **372**, 565 (1980)
- [2] N. Singh, J.H. Evans, *J. Nucl. Mater.* **226**, 277 (1995)
- [3] F.A. Garner, M.B. Toloczko, B.H. Sencer, *J. Nucl. Mater.* **276**, 123 (2000)
- [4] M. Hernández-Mayoral et al., Deliverable D4.9, GETMAT FP7-Project, (2013)
- [5] A. Kohyama, A. Hishinuma, D.S. Gelles, R.L. Klueh, W. Dietz, K. Ehrlich, *J. Nucl. Mater.* **233-237**, 138 (1996)

- [6] L. Malerba, A. Caro, J. Wallenius, *J. Nucl. Mater.* **382**, 112 (2008)
- [7] C. Domain, C. Becquart, J. Foct, *Phys. Rev. B* **69**, 144112 (2004)
- [8] M. Matijasević, E. Lucon, A. Almazouzi, *J. Nucl. Mater.* **377**, 101 (2008)
- [9] R. Krause-Rehberg, H. Leipner, *Positron Annihilation in Semiconductors*; Springer-Verlag, Berlin (1999)
- [10] K. Verheyen, M. Jardin, and A. Almazouzi, *J. Nucl. Mater.* **351**, 209 (2006).
- [11] P. Hautojärvi, *Positrons in Solids, Topics in Current Physics*, Springer, Berlin, vol. 12 (1979)
- [12] P. Horodek, V.A. Skuratov, *Surf. Coat. Technol.* **296**, 65 (2016)
- [13] V. Jansson, L. Malerba, *J. Nucl. Mater.* **443**, 274 (2013)
- [14] V. Jansson, M. Chiapetto, L. Malerba, *J. Nucl. Mater.* **442**, 341 (2013)
- [15] N. Anento, A. Serra, *J. Nucl. Mater.* **440**, 236 (2013)
- [16] D. Terentyev, N. Anento, A. Serra, V. Jansson, H. Khater, G. Bonny, *J. Nucl. Mater.* **408**, 272 (2011)
- [17] C. Becquart, C. Domain, *Nuclear Instruments and Methods in Physics Research Section B: Beam Interactions with Materials and Atoms* **202**, 44 (2003)
- [18] Y. Nagai, Z. Tang, M. Hasegawa, *Radiat. Phys. Chem.* **58**, 737 (2000)